OXFORD

Genetic tuning of β-carotene oxygenase-1 activity rescues cone photoreceptor function in STRA6-deficient mice

Jean Moon, Srinivasagan Ramkumar and Johannes von Lintig (iD)*

Department of Pharmacology, School of Medicine, Case Western Reserve University, Cleveland, OH 44106, USA

*To whom correspondence should be addressed at: Department of Pharmacology (W341), School of Medicine, Case Western Reserve University, 10900 Euclid Avenue, Cleveland, OH 44106, USA. Tel: +1 2163683528; Fax: +1 2163681300; Email: johannes.vonlintig@case.edu

Abstract

Rod and cone photoreceptors in the retina mediate dim light and daylight vision, respectively. Despite their distinctive functions, rod and cone visual pigments utilize the same vitamin A-derived chromophore. To sustain vision, vitamin A precursors must be acquired in the gut, metabolized, and distributed to the eyes. Deficiencies in this pathway in inherited ocular disease states deplete cone photoreceptors from chromophore and eventually lead to cell death, whereas the more abundant rod photoreceptors are less affected. However, pathways that support cone function and survival under such conditions are largely unknown. Using biochemical, histological, and physiological approaches, we herein show that intervention with β-carotene in STRA6-deficient mice improved chromophore supply to cone photoreceptors. Relieving the inherent negative feedback regulation of β-carotene oxygenase-1 activity in the intestine by genetic means further bolstered cone photoreceptor functioning in the STRA6-deficient eyes. A vitamin A-rich diet, however, did not improve cone photoreceptor function in STRA6-deficiency. We provide evidence that the beneficial effect of β-carotene on cones results from favorable serum kinetics of retinyl esters in lipoproteins. The respective alterations in lipoprotein metabolism maintained a steady supply of retinoids to the STRA6-deficient eyes, which ameliorated the competition for chromophore between rod and cone photoreceptors. Together, our study elucidates a cone photoreceptor-survival pathway and unravels an unexpected metabolic connection between the gut and the retina.

Introduction

Visual perception in mammals relies on two types of photoreceptors, with a marked rod or cone-like morphology, existing in the retina (1). Rods are exquisitely sensitive at dim light (scotopic) conditions, whereas cones are critical for color vision under daylight (photopic) conditions (2). Both photoreceptors are distinguished by function, yet they depend on the same vitamin A-derived chromophore (11-*cis*-retinal, 11-*cis*-RAL) for phototransduction (3). Upon light absorption by cone and rod visual pigments, the protein-bound chromophore undergoes a *cis-to-trans* isomerization. The inherent structural change of rod and cone visual pigments triggers G protein-coupled signaling cascades, thereby transducing light to a neuronal signal (4).

The eyes must be supplied with vitamin A for chromophore production and regeneration in the retinal pigment epithelium (RPE) (5). Mammals acquire vitamin A precursors in the intestine and metabolically convert them into retinyl esters (REs) (6). REs circulate in lipoproteins, and the RPE acquires them in a lipoprotein lipase (LPL) dependent manner (7). The liver stores dietary vitamin A and secretes retinol (ROL) bound to the serum retinol binding protein (RBP) (8). The RPE expresses a specific RBP receptor facilitating the uptake of ROL from holo-RBP (9) which is encoded by the stimulated by retinoic acid 6 (*Stra6*) gene (10). Lecithin: retinol-acyltransferase (LRAT) subsequently esterifies ROL to REs (11,12). The RPE protein of 65 kDa (RPE65) converts REs to 11-*cis*-ROL, and RAL dehydrogenase 5 (RDH5) oxidizes 11-*cis*-ROL to the chromophore (13).

Mutations in the genes encoding proteins of ocular retinoid metabolism are associated with a wide range of ocular disease states ranging from complex microphthalmic syndromes to various forms of rod-cone dystrophies (14). Humans with mutations in the *STRA6* gene develop Matthew–Wood syndrome with severe microphthalmia (15). Mice with null mutations in *Stra6* (*Stra6$^{-/-}$*) develop normal eyes, but ocular vitamin A uptake homeostasis is impaired (16). At a young age, *Stra6$^{-/-}$* mice possess significantly lower ocular retinoid concentrations than age-matched wild-type (WT) mice (17). During adolescence, a constant dietary supply with vitamin A increases retinoid concentrations and improves rod functions in the eyes of these mice (18,19). However, the less abundant and unstable cone pigments suffer from chromophore deficiency, and cone function does not recover during aging (19). Similarly, mice with mutations in downstream components of the chromophore production pathway, such as the RPE65 R91W mutant, display mislocalized and dysfunctional cone visual pigments (20,21). The lack of chromophore eventually results in cone cell death and retinal degeneration (22).

A major source of vitamin A in the diet is plant-derived β-carotene (BC) (23). BC is converted to two molecules of retinal (RAL) by the enzyme β-carotene oxygenase-1 (BCO1) (24,25). In clinical trials, dietary BC supplementation with algal preparation presented with beneficial outcomes in patients suffering from retinitis pigmentosa (26,27). Notably, genetic polymorphisms in the *BCO1* gene are associated with macula pigment density and the risk of age-related macular degeneration (28,29), the most

prevalent cone photoreceptor disease (30). Therefore, we sought to study the effects of BC metabolism on cone photoreceptors in biochemical detail using mouse models with impaired cone photoreceptor function.

For this purpose, we took advantage of recently established $Stra6^{-/-}$, $Isx^{-/-}$ and $Stra6^{-/-}$; $Isx^{-/-}$ (DKO) mouse lines (31). Intestine-specific homeodomain transcription factor (ISX) is a transcription factor that mediates the inherent feedback mechanism controlling BCO1 activity in enterocytes of the intestine (32). Compared with WT mice, $Isx^{-/-}$ and DKO mice absorb significantly more BC from the diet and convert it to REs (33). Thus, we analyzed retinal physiology and morphology in these mouse lines under different supply conditions. Our study demonstrated an overall beneficial effect of BC supplementation on retinal physiology. Particularly, BC promoted cone visual pigment maturation and photopic responses in the STRA6-deficient eyes. Our data revealed that differences in serum kinetics of preformed versus BC-derived REs were responsible for the observed rescue of cone photoreceptor function.

Results

Influence of *Isx* and *Stra6* mutations on retinoid biochemistry

We used WT, $Isx^{-/-}$ (34), $Stra6^{-/-}$ (16) and the corresponding $Isx^{-/-}$; $Stra6^{-/-}$ (DKO) (31) double knockout mouse lines in the study. All groups of mice had equal numbers and were on the same C57BL/6 J genetic background. Mice were bred and raised on a vitamin A-rich breeder diet. At the age of 4 weeks, littermates were separated into two groups and subjected to feeding with vitamin A sufficiency (VAS) or BC diet. After 8 weeks of intervention with the two diets, mice were sacrificed in the morning to minimize influences related to circadian rhythmicity (Fig. 1A). For both dietary conditions, we referred to WT as the baseline. We first determined retinoid concentrations in the serum of different mouse lines (Fig. 1 and Supplementary Material, Fig. S1). Eliminating ISX increases BC absorption and conversion (Fig. 1B), and this affected the serum retinoid profile. In a fed state, serum retinol levels remained steady, but REs also existed in $Isx^{-/-}$ mice on a BC diet (Fig. 1C and D). The loss of the *Stra6* gene slightly increased the serum concentration of ROL in $Stra6^{-/-}$ mice (Fig. 1C). DKO mice reflected both the *Stra6* and *Isx* phenotypes, as demonstrated by increased ROL levels under both dietary conditions and increased RE on BC diet (Fig. 1C and D).

The changes in serum retinoid concentrations associated with the *Isx* mutation had no effect on ocular vitamin A uptake homeostasis. $Isx^{-/-}$ mice displayed similar ocular retinoid concentrations as WT mice (Fig. 1E). In contrast, STRA6 was a strong determinant of ocular retinoid homeostasis. Consistent with its role as a vitamin A transporter, STRA6 deficiency caused a sharp decline in ocular retinoid concentration under each dietary condition, except for DKO mice which displayed 3-fold increased ocular retinoid concentration compared to $Stra6^{-/-}$ mice on a BC diet (Fig. 1E).

Retinal morphology of mouse lines

Chromophore deficiency promotes retinal pathologies and is associated with retinal degenerative phenotypes such as Leber congenital amaurosis (35,36) and retinitis pigmentosa (37,38). Thus, we examined retinal morphology of the different mouse lines using optical coherence tomography (OCT), scanning laser ophthalmoscopy (SLO), histological analyses and morphometry

(Fig. 1 and Supplementary Material, Fig. S2). The OCT analyses revealed a normal stratification of the different retinal layers in all mouse lines. Similarly, no morphological alterations were detectable between different genotypes and dietary conditions (Fig. 1G). SLO analyses of $Stra6^{-/-}$ mice revealed bright fluorescent spots in the ventral retina that were not observed in WT and $Isx^{-/-}$ control mice (Fig. 1H). Notably, these spots were also present in DKO mice on VAS diet but were largely absent on BC diet. These spots are characteristic for the activation of microglia and macrophages that migrate to the retina to clear dying retinal cells (39,40). Therefore, we also performed histological analysis of the retinas of different mouse lines, and representative pictures are shown in Supplementary Material, Figure S2. Counting of the photoreceptor nuclei in the outer nuclear layer of the different mouse lines revealed comparable numbers (Supplementary Material, Fig. S2C), which indicates that the fluorescent spots were not associated with photoreceptor degeneration at this age.

BC improves photopic ERG responses in STRA6-deficient eyes

Genotype- and diet-induced changes in visual function were assessed by performing full-field electroretinography (ERG) to record electrical responses of photoreceptors to a light stimulus (41,42) (Fig. 2). Rod-driven scotopic responses (a and b wave amplitudes) were measured in dark-adapted eyes. Across different light intensities, scotopic responses were comparable between WT and $Isx^{-/-}$ mice irrespective of diet (Fig. 2A and C). Similarly, cone-dependent photopic responses (b-wave), measured after light adaptation, were largely indistinguishable between these two groups of mice (Fig. 2B and D).

There was a significant reduction in a- and b-wave amplitudes in $Stra6^{-/-}$ and DKO mice on VAS diet compared with WT and $Isx^{-/-}$ mice. With increasing stimulus intensity, scotopic (Fig. 2E and G) and photopic (Fig. 2F and H) responses were highly dampened. Following BC supplementation, scotopic responses remain-reduced in $Stra6^{-/-}$ mice. Improved photopic responses were noted in the same mice where the ERG b-wave increased in amplitude. On BC diet, DKO mice exhibited significant recovery not only of dark-adapted but also light-adapted ERG responses (Fig. 2G and H).

BC but not preformed vitamin A improves photopic ERG responses in DKO mice

As described before, we observed a remarkable improvement of ERG responses in DKO mice upon feeding with BC. Notably, DKO mice supplemented with BC were not associated with the occurrence of 9-*cis*-RAL, precluding it as a major factor in recovery (Fig. 1F). To further investigate whether this rescue was dependent on BC, we supplied DKO mice with high doses of preformed vitamin A. Adhering to the same regimen of 8 weeks, DKO mice were raised on a chow diet. The standard mouse chow contains around 4-fold higher amounts of vitamin A than the VAS diet (15 vs. 4 IU per gram). As observed in DKO mice raised on a BC diet, the ocular retinoid concentrations of chow-fed DKO mice were about 400 pmol per eye (Supplementary Material, Fig. S3A). Accompanying this increase was a modest improvement in scotopic ERG responses (a- and b-wave) (Supplementary Material, Fig. S3B and D). However, chow diet did not improve photopic responses in DKO mice as BC diet did in their littermates, as displayed by the dampened b-wave amplitudes in ERG recordings (Fig. 2F and H and Supplementary Material, Fig. S3C and E).
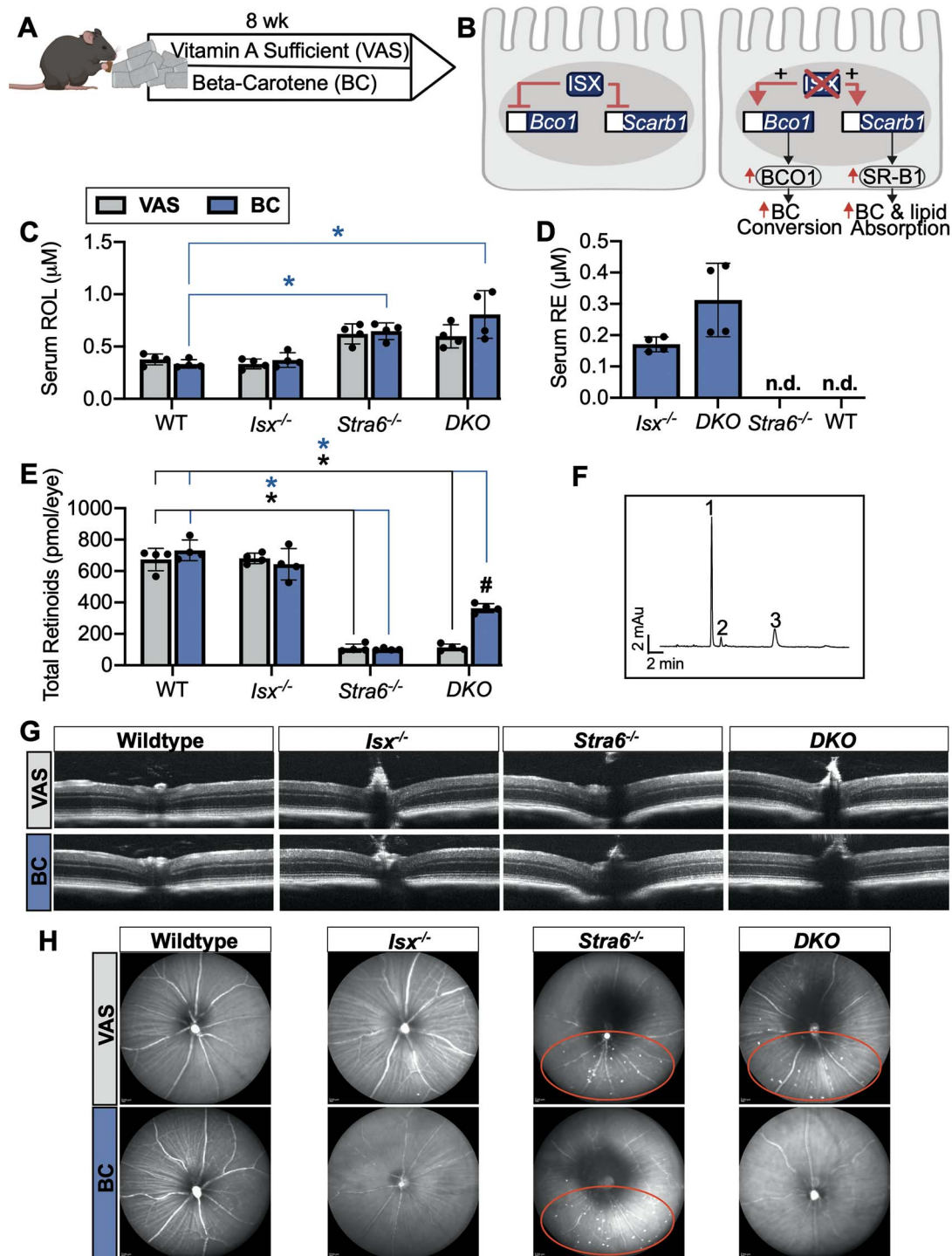
Figure 1. Characterization of mouse models. (**A**) After weaning (4 weeks), four groups of mice (WT, $Isx^{-/-}$, $Stra6^{-/-}$, DKO) were fed a diet that was supplemented with either preformed vitamin A (4000 IU/kg; VAS) or β-carotene (25 mg/kg; BC) for 8 weeks. (**B**) ISX represses expression of $Bco1$ and $Scarb1$. Knocking out Isx results in increased BC conversion and absorption. At the end of the dietary intervention, serum (**C**, **D**) and ocular (**E**) retinoid concentrations were determined by HPLC. (**F**) Representative HPLC trace from dark-adapted eyes of DKO mice fed BC. The structure of the retina was examined, and the representative OCT (**G**) and SLO (**H**) images were collected. The circles mark regions with autofluorescent spots. 1: 11-*cis*-retinal-oxime (syn); 2: all-*trans*-retinal-oxime (syn); 3: 11-*cis*-retinal-oxime (anti); Isx: Intestine-specific homeobox transcription factor; $Bco1$: β-carotene oxygenase 1; $Scarb1$: scavenger receptor class B member 1; RE: retinyl esters; ROL: retinol. n.d.: not detected. $*$ $P < 0.05$ between genotype; # $P < 0.05$ VAS versus BC, within genotype.

BC diet recovers cone opsin expression in the STRA6-deficient eyes

Rod and cone photoreceptors express specific opsins, rhodopsin (encoded by Rho gene) in rods, and M-opsin (encoded by the $Opn1mw$ gene) and S-opsin (encoded by the $Opn1sw$ gene) in cones

(43). We determined the mRNA expression levels of the respective genes in the eyes of the different mouse lines. We observed no effects of the Isx mutation on Rho expression. In contrast, mRNA levels in $Stra6^{-/-}$ and DKO mice were $\sim 50\%$ compared to that of age-matched WT mice on VAS diet (Fig. 3A). We obtained
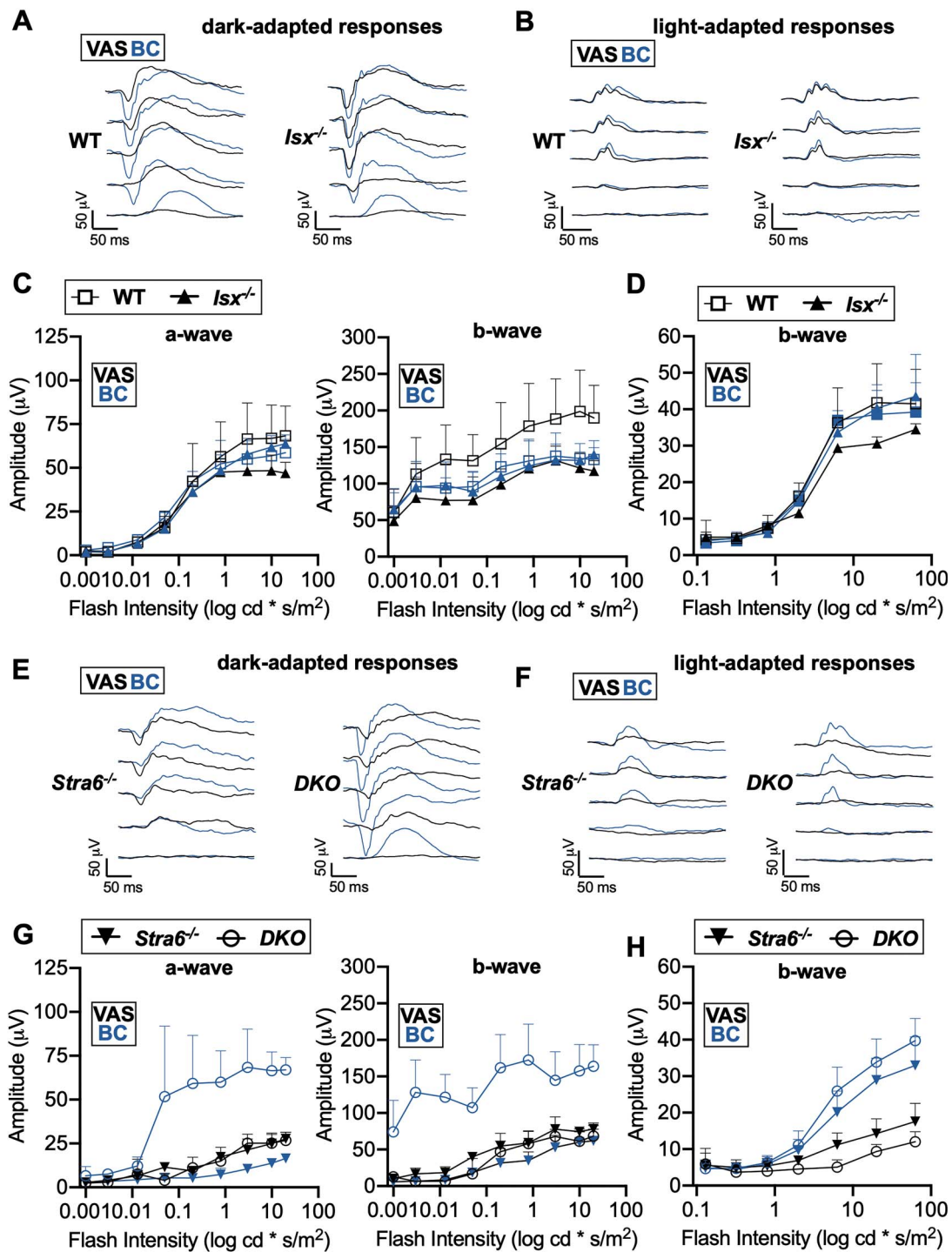
Figure 2. Measuring impact of diet and genotype on visual function. ERG was performed on all groups of mice maintained on either VAS or BC diets for 8 weeks. Scotopic responses were recorded after a 16 h dark adaptation. Photopic responses were collected after a 7 min light adaptation. ISX deficiency did not impact retina function. The representative dark-adapted traces (**A**) and (**C**) mean (±SD) a-wave and b-wave amplitudes as well as light-adapted traces (**B**) and (**D**) mean (±SD) b-wave amplitude from WT and *Isx*$^{-/-}$ mice. *Stra6*$^{-/-}$ mice have significantly reduced visual responses. The representative dark-adapted traces (**E**) and (**G**) mean (±SD) a-wave and b-wave amplitudes as well as light-adapted traces (**F**) and (**H**) mean (±SD) b-wave amplitude from *Stra6*$^{-/-}$ and *DKO* mice.

comparable results with ocular RNA preparation of the different mouse lines subjected to BC diet feeding. However, consistent with the increased ocular retinoid concentrations, *Rho* mRNA expression increased in *DKO* mice under this diet (Fig. 3A). Additionally, we analyzed the expression of G protein subunit alpha transducin 1 (*Gnat1*) which is integral, specifically, to rod specific components of phototransduction (Fig. 4A). The expression of *Gnat1* mirrored the expression of the *Rho* gene. Based on the immunostaining of the retinal sections, Rhodopsin protein was detected in all analyzed retinas, though the staining appeared to be lower in *Stra6*$^{-/-}$ and *DKO* mice than in WT mice (Fig. 3D–G).
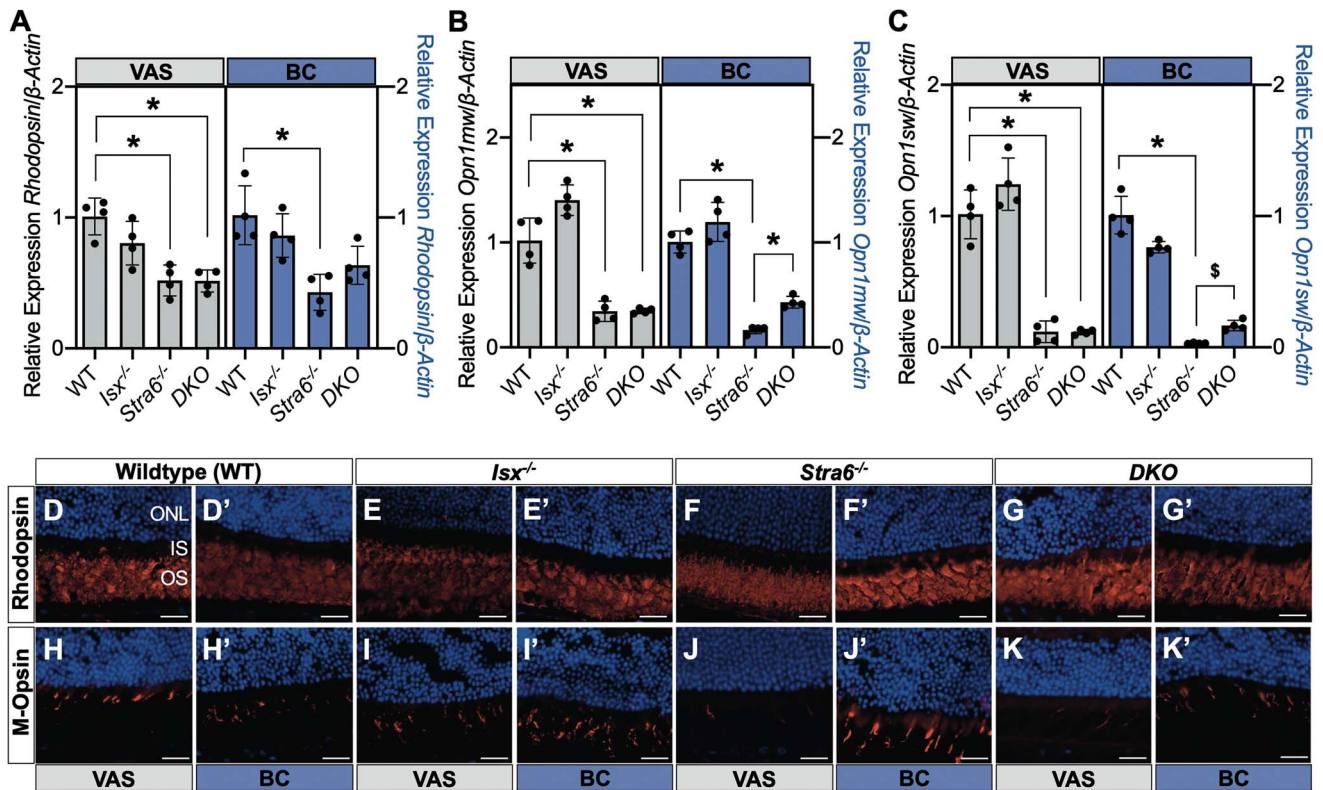
Figure 3. Rod and cone opsin expression. *Rhodopsin* (**A**), *Opn1mw* (**B**) and *Opn1sw* (**C**) gene expression was determined by quantitative RT-PCR. Values (mean ± SD) were normalized to β-actin. Representative retinal cross sections with Rhodopsin and M-opsin immunolabeling (**D,D'–G,G'** and **H,H'–K,K'**). Scale bar indicates 25 μm. ∗ $P < 0.05$ between genotype on the same diet by one-way ANOVA analysis. \$ $P < 0.05$ between *Stra6*$^{-/-}$ and *DKO* mice on the BC diet by unpaired t-test.

The expression levels of *Opn1mw* and *Opn1sw*, encoding respectively M- and S-opsin, were lower in *Stra6*$^{-/-}$ and *DKO* mice than in WT and *Isx*$^{-/-}$ mice under both dietary conditions (Fig. 3B and C). Notably, BC diet feeding increased *Opn1mw* mRNA in *DKO* mice (Fig. 3B). Again, the *Isx* genotype alone had no effect on the expression levels of the cone opsins. The expression of *Gnat2* mRNA, encoding a key component of the cone phototransduction cascade, resembled this expression pattern with a significant increase in *DKO* mice subjected to BC diet feeding (Fig. 4B). Accordingly, staining for M-opsin was barely detectable in retinal sections of *Stra6*$^{-/-}$ mice and *DKO* mice on VAS diet. In contrast, significant staining for the M-cone opsin became detectable in *Stra6*$^{-/-}$ mice and *DKO* mice on BC diet (Fig. 3H–K). To exclude that retinal sectioning affected the evaluation of the expression of M-cone opsin, we repeated the staining in whole mount retinas from different mouse lines and dietary conditions. As depicted in Supplementary Material, Figure S4, the results recapitulated the outcomes from the analyses in retinal sections. WT and *Isx*$^{-/-}$ mice showed strong staining of M-opsin independent of the diet. The dietary intervention had a significant effect in *Stra6*$^{-/-}$ and *DKO* mice. Although M-opsin staining was barely detectable on VAS diet, we observed staining for M-opsin in retinas of mice subjected to BC diet that was particularly strong in *DKO* mice.

BC diet affects serum RE kinetics and ocular *Lpl* expression

We noted a beneficial effect of BC feeding on the physiology of the *Stra6*$^{-/-}$ and *DKO* mice retinas. Gene expression of proteins involved in ocular retinoid metabolism within the RPE, *Lrat* and *Rpe65*, remained largely unaffected by diet or genotype

(Fig. 4C and D) (11,44). It has been previously reported that *BCO1* is expressed at high levels in the RPE of the human eyes (45,46). To examine whether the beneficial effect of BC supplementation results from an eye-specific conversion of BC to retinoids, we performed quantitative real-time PCR (qRT-PCR) analysis for genes encoding scavenger receptor class B type 1 (SR-B1) which facilitates the uptake of carotenoids (47) and BCO1 which converts BC to RAL (24). On VAS diet, the expression of the two genes was comparable in the eyes of all mouse lines. Markedly, *Bco1* mRNA levels were very low and displayed a C_t value >30 in ocular RNA preparation, suggesting that the gene is expressed at marginal levels or in very few cell types on the eyes (Fig. 5A). On BC diet, the expression levels remained extremely low for *Bco1* in all genotypes, but there was a significant increase in *Scarb1* mRNA levels in *Isx*$^{-/-}$ mice but not in the *DKO* mice (Fig. 5A and B). Since no BC was detectable in the eyes or serum and ocular *Bco1* expression was very low, we rather exclude that an eye-specific conversion contributed to the improvement.

We next examined the expression levels of genes involved in vitamin A uptake from RBP or lipoproteins in the eye. *Stra6* mRNA expression was comparable in WT and *Isx*$^{-/-}$ mice and not detectable in *Stra6*$^{-/-}$ and *DKO* mice (Fig. 5C). The mRNA levels of LPL, which is involved in ROL uptake from circulating lipoproteins, were comparable on VAS diet (7,48). Interestingly, *Lpl* mRNA expression was higher in *DKO* mice fed BC diet than in other mouse genotypes (Fig. 5D).

In consideration of the role LPL has in acquiring vitamin A from circulating lipoproteins and of previous reports that BC affects lipoprotein metabolism and vitamin A transport, we considered whether BC influences intestinal lipoprotein metabolism (48–50). Prior to being incorporated into chylomicrons, vitamin A is
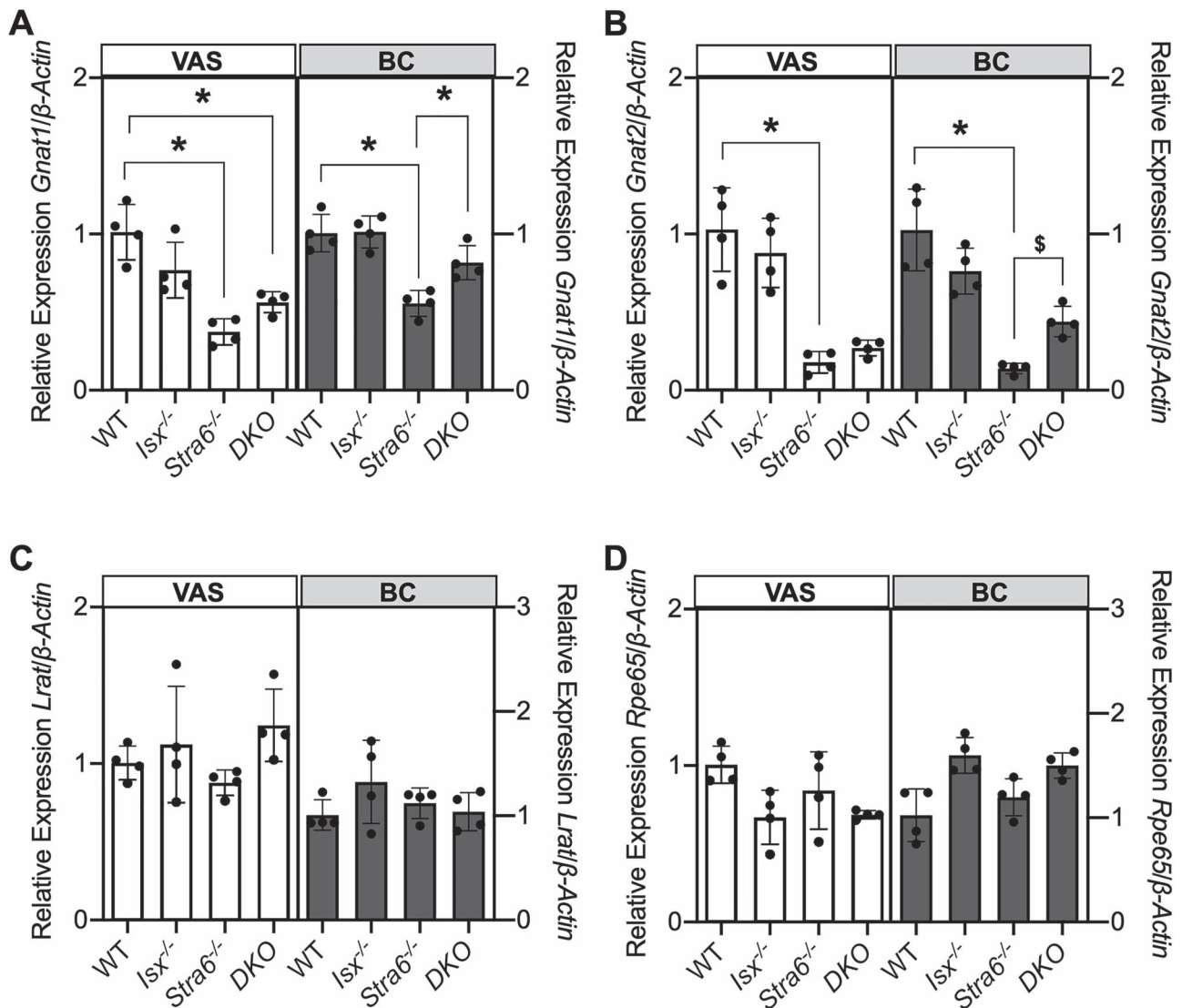
Figure 4. Expression of visual cycle and phototransduction genes. Quantitative RT-PCR analysis of rod (**A**) and cone (**B**) specific transducin alpha subunits. Gene expression of visual cycle genes *Lrat* (**C**) and *Rpe65* (**D**). Values (mean ± SD) were normalized to β-actin. ∗ $P < 0.05$ between genotype on the same diet by one-way ANOVA analysis. $ $P < 0.05$ between *Stra6*$^{-/-}$ and *DKO* mice on the BC diet by unpaired t-test.

esterified by the endoplasmic reticulum resident enzyme LRAT (51). *Lrat* mRNA expression was more than 4-fold increased DKO mice on BC diet when compared with WT mice (Fig. 5E). Chylomicron assembly is critically dependent on apo-lipoprotein B (ApoB) and the chaperone microsomal triglyceride transfer protein (MTP). qRT-PCR analysis with RNA preparations of jejunum revealed a significant increase of *Mttp* expression in BC fed DKO mice (Fig. 5F). *Apob* followed a similar trend though the difference was not significant (Fig. 5G). Thus, altered expression of genes associated with lipoprotein metabolism on BC diet may well contribute to the high levels of serum RE in the fed state (Fig. 1D). To analyze whether RE also exists in the postprandial circulation, we determined serum RE in starved *DKO* mice. As shown in Supplementary Material, Figure S5, significant amounts of RE were present in the postprandial circulation of these mice.

The effect of BC on retinal physiology is light independent

We next examined the role of putative light-dependent formation of chromophore for cone photoreceptors. To analyze the

contribution of these retinal G protein-coupled receptor (RGR)-dependent pathways for chromophore production (52,53), we reared WT, *Stra6*$^{-/-}$, and *DKO* mice on VAS or BC diet in darkness. After 8 weeks, we measured scotopic and photopic responses of the retina of these mice (Supplementary Material, Fig. S6). On VAS diet, the ERG responses were significantly lower in *Stra6*$^{-/-}$ and *DKO* mice under both scotopic and photopic conditions (Supplementary Material, Fig. S6A and B). BC feeding increased scotopic responses of *DKO* mice more than that of *Stra6*$^{-/-}$ mice (Supplementary Material, Fig. S6C). Photopic responses in *DKO* mice again reached WT levels (Supplementary Material, Fig. S6D), indicating their improvement was not light-dependent.

BC feeding increases the concentration of liganded opsin in *DKO* mice

Previously, we reported that STRA6-deficient eyes display significant amounts of unliganded opsins even when supplemented with a vitamin A-rich diet during adolescence (19). It is widely accepted that unliganded opsin activates the phototransduction cascade even in darkness (36). Constitutive activity of unliganded
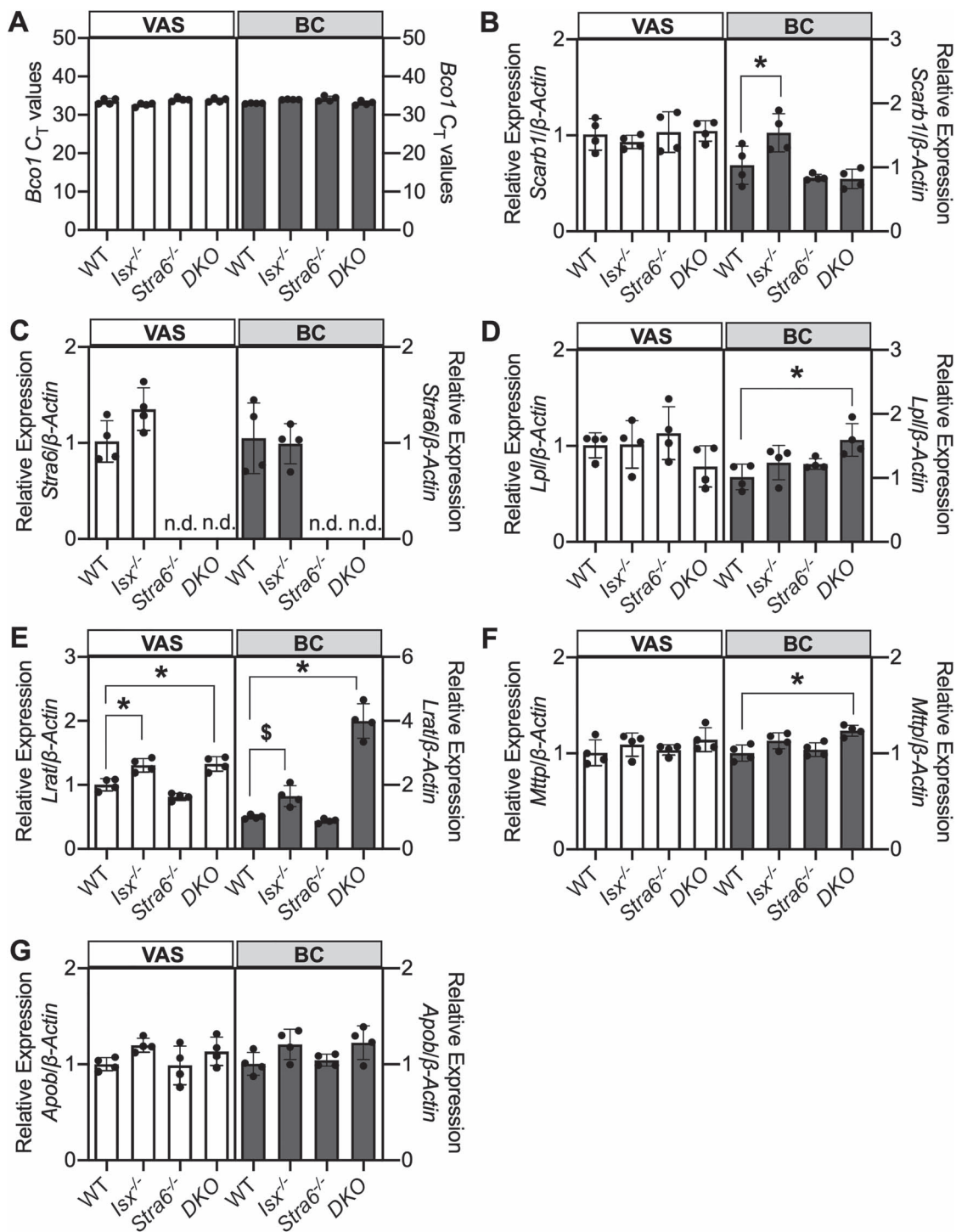
Figure 5. Expression of vitamin A uptake and metabolism-related genes. Gene expression analyses were performed in ocular tissues (**A–D**) and small intestine (**E–G**) after VAS or BC supplementation. Raw *Bco1* C_T values (A) and *Scarb1* (B), *Stra6* (C), and *Lpl* (D) expression in the eyes. *Lrat* (E), *Mttp* (F), and *Apob* (G) expression in the jejunum. Relative expression (mean ± SD) represent values normalized to β-actin. n.d.: not detected. ∗ $P < 0.05$ between genotype on the same diet. $ $P < 0.05$ between WT and $Isx^{-/-}$ mice on the BC diet by unpaired t-test.

rod opsin is equivalent to that of background light and results in a concurrent reduction in phototransduction gain. To determine the amount of unliganded opsins in photoreceptors of *DKO* mice, we supplemented dark-adapted *DKO* and WT mice with the chromophore 9-*cis*-RAL (Fig. 6A). This chromophore surrogate can occupy the binding pocket of unliganded rod and cone opsins, and its ocular accumulation is a measure for the presence of unliganded opsins in photoreceptor cells. Following supplementation,

we detected significant amounts of 9-*cis*-RAL in HPLC analysis of the eyes of *DKO* mice on VAS diet (Fig. 6B). Small amounts of 9-*cis*-RAL were detected in *DKO* mice on BC diet and in WT mice raised under both dietary conditions, indicating that the large majority of opsin existed in the liganded form in dark-adapted eyes of these mice (Fig. 6B and C). Thus, BC feeding rescued the imbalances between opsin expression and chromophore levels brought up by mutations in the *Stra6* gene in *DKO* mice. This
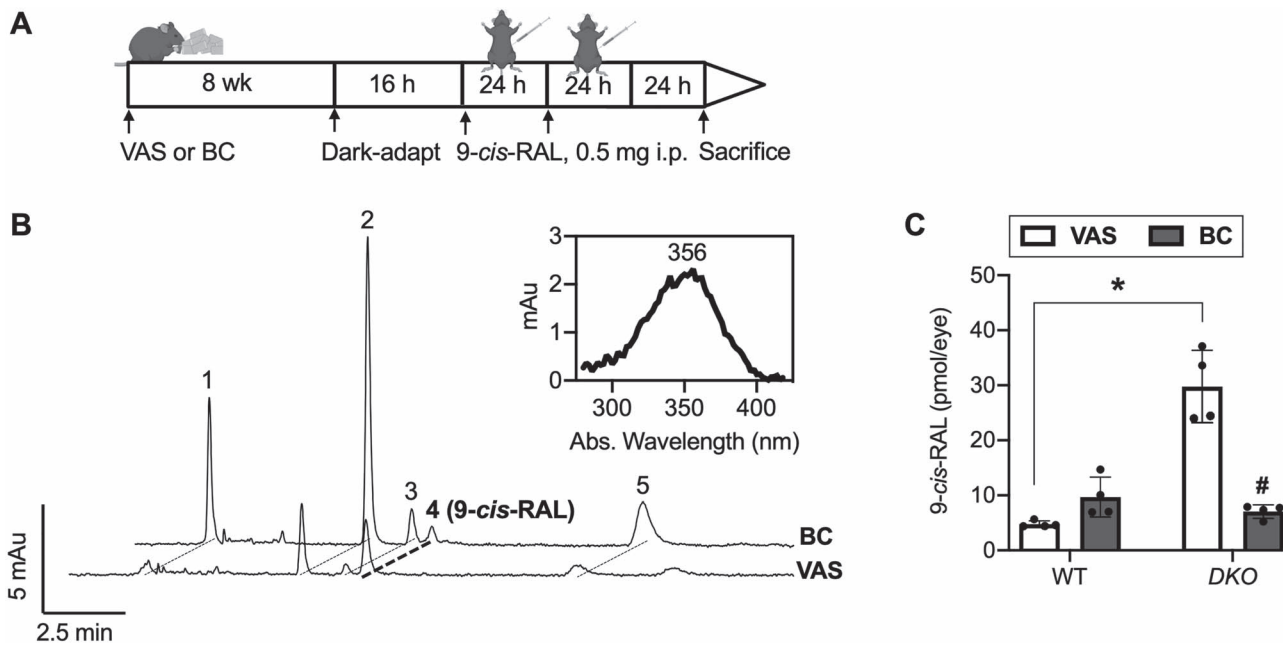
Figure 6. BC-supplemented DKO mice possess lower levels of free unliganded opsin. Mice, supplemented with vitamin A sufficient or β-carotene diet, were injected with 9-*cis*-RAL intraperitoneally twice (24 h interval) after dark adaptation (**A**). Representative HPLC trace and spectrum of 9-*cis*-RAL oxime peak (**B**). Quantification of 9-*cis*-RAL content (**C**). 1: retinyl esters; 2: 11-*cis*-retinal-oxime (syn); 3: all-*trans*-retinal-oxime (syn); 4: 9-*cis*-retinal; 5: 11-*cis*-retinal-oxime (anti). $*\,P < 0.05$ between genotype on the same diet; $\#\,P < 0.05$ VAS versus BC, within genotype.

observation accounted for the significant improved scotopic and photopic ERG responses of this mouse line on BC diet.

Discussion

To establish and sustain vision, dietary retinoid precursors are absorbed in the intestine, transported in the body, taken up by cells of the RPE, and metabolized to chromophore (5). Ocular disease states ranging from nutritional vitamin A deficiency to various forms of inherited retinal dystrophies are associated with this pathway (14). Mouse models for such diseases are characterized by cone photoreceptors that are depleted of chromophore (20). This chromophore deficiency causes oxidative stress and eventually cone photoreceptor cell death that can culminate in vision loss (22). We here observed that supplementation with BC had a favorable effect on cone photoreceptor biology in mice suffering from impaired ocular vitamin A uptake homeostasis. Retinal function of these mice was further improved when the inherent negative feedback control of BC absorption and metabolism at the intestine was genetically abolished through *Isx* gene knockout (32,54). ISX is a homeodomain transcription factor that, in response to retinoic acid signaling, suppresses the expression of the *Scarb1* and *Bco1* gene in enterocytes of the intestine (32,55). This control mechanism is particularly stringent in mice where the large majority of BC is converted to retinoids in enterocytes of the intestine (55). Humans absorb significantly more BC, and the human circulation displays significant higher amounts of the provitamin than rodents (56). BC supplementation increased the ocular concentrations of retinoids in *DKO* mice (Fig. 1E). More importantly, this was complemented with an overall beneficial effect on cone photoreceptor function (Fig. 2). The expression levels of genes encoding the M- and S-cone opsins were augmented compared with that of mice supplemented with preformed vitamin A alone. The *Gnat2* gene followed a similar trend, and this improvement was accompanied by the occurrence of mature

cone pigments in the retinas of BC supplemented *Stra6*^{-/-} and *DKO* mice (Figs 3 and 4). The latter conclusion stemmed from immunohistochemically staining for M-opsin in these mice as well as from measurable ERG responses to light under photopic conditions. The improvement of the photopic responses, which was dependent on BC diet, was observed in both *Stra6*^{-/-} and *DKO* mice. Remarkably, the analyses in *DKO* mice showed that the recovery of photopic responses in *DKO* mice was not simply a function of ocular retinoid concentration. *DKO* mice raised on chow diet also displayed significantly higher ocular retinoid concentrations than *DKO* mice on VAS diet. Despite ocular retinoid concentrations being comparable to BC supplemented *DKO* mice, photopic responses to light were still reduced. In fact, we previously reported in *Stra6*^{-/-} mice that even after prolonged feeding with chow diet, photopic ERG responses to light remain impaired though scotopic ERG responses increased. This phenotype was associated with the absence of cone pigments in immunostainings of the retina (19).

Our findings raise the question about the biochemical and molecular basis of the cone-specific improvements upon BC supplementation. It has been reported that cone specific pathways for chromophore generation exist in the eyes (57). Therefore, we speculated that eye-specific conversion of BC delivers precursors for these pathways. However, consistent with previous reports (58), *Bco1* mRNA was very low in qRT-PCR analysis of the eyes of *DKO* and other mice in this study (Fig. 5). We want not to exclude that *Bco1* mRNA in total ocular RNA preparations is particularly low because the gene only is expressed in specific cell types, i.e. Muller glial cells. However, the lack of BC in the circulation makes an eye-specific BC conversion rather unlikely. We also examined whether light-dependent pathways for chromophore production/regeneration contributed to the improvement of cone vision upon BC supplementation (52). However, *DKO* mice raised in either darkness or light displayed similar scotopic and photopic ERG responses (Supplementary Material, Fig. S6). We additionally considered whether 9-*cis*-RAL production from BC contributed to

the improved cone function of *DKO* mice. The absence of significant amounts of 9-*cis*-retinoid diastereomers in the circulation and in ocular tissues suggested that this production did not contribute to the improvement of cone physiology in *DKO* mice (Fig. 1F). In fact, previous reports indicate that poor absorption of 9-*cis*-BC as well as intrinsic isomerase activity of BCO1 prevent generation of the 9-*cis*-RAL diastereomers in mice (59,60).

Thus, another mechanism must account for the improved cone functioning of *DKO* mice on BC diet. Mice deficient for STRA6 and its binding protein RBP rely on an ocular delivery of vitamin A in the form of REs (7,17). When subjected to dietary vitamin A deprivation, STRA6-deficient eyes have limited chromophore (18). In mice, REs mainly exist in the postprandial circulation transiently (61). Our study now reveals that this phenomenon changed under conditions of BC supplementation in ISX-deficiency. The enhanced absorption and conversion of BC to retinoids led to altered RE kinetics in the circulation. This alteration was driven by altered expression of genes encoding LRAT and MTP in the intestine which catalyzes RE formation and regulates chylomicron assembly, respectively. Such a phenomenon where BC impacts lipoprotein metabolism has also been reported previously at the fetal–maternal barrier (50). REs were present in the fed state but also in the starved state, indicating that this form of vitamin A existed in several lipoprotein classes under this condition. The altered plasma kinetics of REs resulted in a steady supply of retinoids to the eyes in *DKO* mice on BC diet. We suggest that this constant and steady supply increased ocular retinoid concentration and enabled cones to compete with rods for chromophore. Cone pigments are unstable and can decay into chromophore and free opsin. This characteristic of cone pigments, which are surrounded by a vast majority of rod photoreceptors, may result in a constant 'stealing' of chromophore in a vitamin A deficient retina (20). Cone photoreceptor functioning improved, as seen by the absence of unliganded opsins in the retinas of these mice (Fig. 6). Our study suggests that altered RE kinetics are a significant contributor for the improved cone function in *DKO* mice and to a lesser extent in *Stra6*$^{-/-}$ mice, but we do not want to exclude involvement from other mechanisms.

BC feeding did not only improve cone photoreceptor maturation and function but also had an appreciable effect on the fluorescent spots that were noted in fundus images from *Stra6*$^{-/-}$ mice on both diets as well as from *DKO* mice on a VAS diet (Fig. 1H). Many studies reported that chromophore deficiency of cone photoreceptors leads to cell death and irreversible loss of sight (14). In fact, mice deficient for STRA6 and its ligand RBP have both been reported to show signs of retinal degeneration while aging (19,62). Therefore, we conclude that the improved cone function upon BC supplementation has profound effects on retinal health in these animals.

Collectively, our data unraveled a yet underappreciated role of BC for vision. BC promoted cone photoreceptor function and maintenance in the STRA6-deficient mouse eyes. This effect was not likely achieved by a local conversion and metabolism of BC in the eye, but rather by changes in lipoprotein metabolism and kinetics of serum RE. Interestingly, studies administering labeled vitamin A in volunteers demonstrated that preformed vitamin A and vitamin A derived from BC display different plasma kinetics upon supplementation (46). Clinical studies have also shown that supplementation with BC extracts had favorable effects in retinitis pigmentosa patients (26). Notably, genetic polymorphisms in the *BCO1* gene have been associated with AMD (28,29). Previously, this association was explained by interactions between BC and macula pigments during absorption and transport (30).

Our findings now indicate that increased BCO1 activity has a direct and beneficial effect on cone photoreceptors. Therefore, the association between BCO1 and ocular disease states warrants further investigations.

Materials and Methods
Animals, housing and diets
Female mice on a C57BL/6 J genetic background were used for this study. As previously described, mice expressing a mutant *Stra6* or *Isx* allele were generated (16,34). *Isx*$^{-/-}$; *Stra6*$^{-/-}$ double knockout (*DKO*) mice were generated in the vivarium at Case Western Reserve University (31). WT mice were acquired from the Jackson Laboratory. Light-reared mice were housed on a 12:12 h light/dark cycle, and dark-reared mice were housed in a dark room with ad libitum access to food and water. All mice were bred and raised on a standard rodent chow diet consisting of 15 000 IU vitamin A/kg diet (Prolab RMH 3000, LabDiet, St. Louis, MO, USA). At the time of weaning, mice were maintained on a diet supplemented with vitamin mix V13002 (4000 IU vitamin A, retinyl acetate) (VAS diet) or BC (25 mg/kg; ∼7000 IU retinol assuming 1 μg RAE:12 μg BC) (BC diet) for 8 weeks. Special diets were prepared by Research Diets (New Brunswick, NJ, USA). At the end of the dietary intervention, fed- or 16 h fasted mice were anesthetized using a drug cocktail of ketamine (60 mg/kg) and xylazine (5 mg/kg). Blood samples were collected via cardiac puncture. Mice were transcardially perfused with PBS and then sacrificed by cervical dislocation. The eyes were immediately harvested for analysis or snap-frozen in liquid nitrogen and stored at −80°C until further use. All mice experiments in these studies were conducted in accordance with protocols approved by Case Western Reserve University Institutional Animal Care and Use Committee.

HPLC retinoid analyses
Retinoids were extracted from serum (100 μl) or one entire eyecup as previously described (31). In brief, sera and eyecups were homogenized in a final 200 μl volume with either PBS or 2 M hydroxylamine (pH 6.8), respectively. Retinoids were then extracted two times using a mixture of 200 μl methanol, 400 μl acetone and 500 μl hexane. A normal-phase Zorbax Sil (5 μm, 4.6 × 150 mm) column was used for HPLC analysis. Chromatographic separation was achieved by isocratic flow of 10% ethyl acetate/90% hexanes. To quantify the molar amounts of retinoids, the HPLC was previously calibrated with synthetic standard compounds.

SD-OCT and fundus imaging
Four to five mice were assessed at a time. Prior to the eye examination, 1% tropicamide (Bausch and Lomb, Tampa, FL, USA) was used to dilate the pupils. Mice were anesthetized by intraperitoneal injection of ketamine/xylazine rodent cocktail. Spectral domain optical coherence tomography (SD-OCT, Bioptigen) images were positioned to adjust the optic nerve in the center. B-scan images were acquired and averaged using the Bioptigen software. Confocal scanning laser ophthalmoscope (SLO Spectralis HRA2, Heidelberg Engineering, Heidelberg, Germany) was used to collect mouse fundus images. The fundus camera was aligned to the pupil using the near infrared reflective laser (820 nm) to obtain evenly illuminated fundus images.

Histology
Histological analyses were performed using eyes enucleated from mice following perfusion. The eyes were fixed in 4%

paraformaldehyde overnight at room temperature. Paraffin embedding, sectioning (10 μm), and hematoxylin and eosin (HE) staining were conducted by the Visual Sciences Research Center Core at Case Western Reserve University. The HE-stained sections were imaged using the Leica DM600 microscope.

Electroretinography

Light-reared mice were dark adapted overnight prior to examination. Pupils were dilated using 1% tropicamide (Bausch and Lomb), and mice were anesthetized by an intraperitoneal injection of ketamine/xylazine rodent cocktail. Mice were placed on a heating pad throughout the recording session to keep the body temperature at 37°C. Ag-AgCl electrodes were placed on the surface of the cornea (Diagnosys Celeris, Lowell, MA). For dark-adapted ERG responses, mice were exposed to 10 steps of a white light, flash stimulus ranging from 0.001 to 20 cd s $\times$ m^{-2}. Interstimulus intervals were set at 4 s for low-luminance flashes and 90 s for the highest stimulus. For cone ERG responses, mice were exposed to a steady adapting light field for 7 min, and waveforms were recorded with strobe-flash stimuli (0.32 to 63 cd s $\times$ m^{-2}) superimposed on the adapting field. Amplitude values were averaged between left and right eyes.

9-cis-retinal administration

WT and *DKO* mice, dark adapted for 16 h, were injected intraperitoneally with 0.5 mg 9-*cis*-retinal (Cayman Chemicals, Ann Arbor, MI, USA) or DMSO vehicle daily for two consecutive days. Mice were euthanized 24 h post-treatment. The eyes were enucleated, and 9-*cis*-retinal concentrations were determined by HPLC.

Retina immunohistochemistry

Following euthanasia, the eyes were immediately harvested. For frozen retinal cross-sections, the eyes were fixed in 4% paraformaldehyde overnight. Samples were embedded in OCT and sectioned (5 μm) at the Visual Sciences Research Center Core at Case Western Reserve University. Retinal sections were thawed to room temperature, rehydrated with PBS and blocked using 4% normal goat serum. The sections were incubated with 1:500 monoclonal 1D4 anti-rhodopsin (Dr Robert Molday, University of British Columbia, Canada) and 1:250 anti-M opsin (cat no. AB5405, Millipore Sigma, St. Louis, MO, USA) primary antibody overnight at 4°C and then washed with PBST (0.1% TritonX-100 in PBS). Alexa fluor 555 was used as the secondary antibody at a 1:500 dilution. The sections washed with PBST and then PBS before mounting. For retinal whole mounts, the eyes were fixed in 4% paraformaldehyde for 1 h. To track orientation, the inferior side of the eye was marked. The cornea was excised, and the lens and vitreous were both removed. Radial incisions were made to flatten the eyecup. The retinal layer was separated from the posterior eyecup (RPE and sclera). After washing the retinal tissue with PBST, ice-cold methanol was added in a dropwise manner for permeabilization. The retina was further flattened between two coverslips in 4% paraformaldehyde and then incubated with M-opsin (cat no. AB5405, Millipore Sigma) primary antibody (1:250) overnight at 4°C. The flatmounts were washed with PBST before being incubated with an Alexa fluor 555 secondary antibody (1:500) for 2 h at room temperature. Following PBST washes, the flatmounts were mounted on microscope slides with the photoreceptor side facing up. Images were acquired by the Hamamatsu NanoZoomer slide scanner at the Case Western Reserve University Light Microscopy Core.

Quantitative real-time PCR

Total RNA was extracted from enucleated eyes using the TRIzol method (Invitrogen, Carlsbad, CA, USA). The Nano drop ND-1000 spectrophotometer (Thermo Fisher Scientific, Waltham, MA, USA) was used to quantify RNA, and cDNA was generated using the High Capacity RNA to cDNA kit (Applied Biosystems, Thermo Fisher Scientific). RT-PCR was carried out using the TaqMan Master Mix (Applied Biosystem; Thermo Fisher Scientific) and primers (Applied Biosystems) to amplify *β-actin* (Mm02619580), *Apob* (Mm01545159), *Bco1* (Mm01251350), *Gnat1* (Mm01229120), *Gnat2* (Mm00492394), *Lpl* (Mm00434764), *Lrat* (Mm00469962), *Mttp* (Mm004435015), *Opn1mw* (Mm00433560), *Opn1sw* (Mm00432058), *Rho* (Mm01184405), *Rpe65* (Mm00504133), *Scarb1* (Mm00450234) and *Stra6* (Mm00486457). Gene expression levels were normalized to the expression of housekeeping gene *β-actin* using the $\Delta\Delta$Ct method.

Statistical analysis

All statistical analyses were performed Graphpad Prism 8.0 software. One-way ANOVA was applied for comparisons made between genotypes, and two-way ANOVA was used when the measured response is affected by both diet and genotype. The Tukey multiple-comparisons post hoc tests were carried out. An alpha level of $P < 0.05$ was considered significant. Data are expressed as mean values $\pm$ standard deviation. An $n = 4$ refers to four individual mice in ERG tests or four individual eyes from unique mice.

Supplementary Material

Supplementary Material is available at *HMG* online.

References

1. Kiser, P.D., Golczak, M. and Palczewski, K. (2014) Chemistry of the retinoid (visual) cycle. *Chem. Rev.*, **114**, 194–232.
2. Rodieck, R.W. (1998) *The First Steps in Seeing*. Sinauer Associates, Sunderland, MA.
3. Goldsmith, T.H. (2013) Evolutionary tinkering with visual photoreception. *Vis. Neurosci.*, **30**, 21–37.
4. Burns, M.E. and Baylor, D.A. (2001) Activation, deactivation, and adaptation in vertebrate photoreceptor cells. *Annu. Rev. Neurosci.*, **24**, 779–805.
5. von Lintig, J., Moon, J. and Babino, D. (2021) Molecular components affecting ocular carotenoid and retinoid homeostasis. *Prog. Retin. Eye Res.*, **80**, 100864.
6. Blaner, W.S., Li, Y., Brun, P.J., Yuen, J.J., Lee, S.A. and Clugston, R.D. (2016) vitamin a absorption, storage and mobilization. *Subcell. Biochem.*, **81**, 95–125.

7. Quadro, L., Blaner, W.S., Salchow, D.J., Vogel, S., Piantedosi, R., Gouras, P., Freeman, S., Cosma, M.P., Colantuoni, V. and Gottesman, M.E. (1999) Impaired retinal function and vitamin A availability in mice lacking retinol-binding protein. *EMBO J.*, **18**, 4633–4644.

8. Blaner, W.S., Hendriks, H.F., Brouwer, A., de Leeuw, A.M., Knook, D.L. and Goodman, D.S. (1985) Retinoids, retinoid-binding proteins, and retinyl palmitate hydrolase distributions in different types of rat liver cells. *J. Lipid Res.*, **26**, 1241–1251.

9. Bok, D. and Heller, J. (1976) Transport of retinol from the blood to the retina: an autoradiographic study of the pigment epithelial cell surface receptor for plasma retinol-binding protein. *Exp. Eye Res.*, **22**, 395–402.

10. Kawaguchi, R., Yu, J., Honda, J., Hu, J., Whitelegge, J., Ping, P., Wiita, P., Bok, D. and Sun, H. (2007) A membrane receptor for retinol binding protein mediates cellular uptake of vitamin a. *Science*, **315**, 820–825.

11. Batten, M.L., Imanishi, Y., Maeda, T., Tu, D.C., Moise, A.R., Bronson, D., Possin, D., Van Gelder, R.N., Baehr, W. and Palczewski, K. (2004) Lecithin-retinol acyltransferase is essential for accumulation of all-trans-retinyl esters in the eye and in the liver. *J. Biol. Chem.*, **279**, 10422–10432.

12. Amengual, J., Golczak, M., Palczewski, K. and von Lintig, J. (2012) Lecithin:retinol acyltransferase is critical for cellular uptake of vitamin A from serum retinol-binding protein. *J. Biol. Chem.*, **287**, 24216–24227.

13. Kiser, P.D. (2022) Retinal pigment epithelium 65 kDa protein (RPE65): an update. *Prog. Retin. Eye Res.*, **88**, 101013.

14. Kiser, P.D. and Palczewski, K. (2016) Retinoids and retinal diseases. *Annu. Rev. Vis. Sci.*, **2**, 197–234.

15. Chassaing, N., Ragge, N., Kariminejad, A., Buffet, A., Ghaderi-Sohi, S., Martinovic, J. and Calvas, P. (2012) Mutation analysis of the STRA6 gene in isolated and non-isolated anophthalmia/microphthalmia. *Clin. Genet.*, **9999**, 244–250.

16. Ruiz, A., Mark, M., Jacobs, H., Klopfenstein, M., Hu, J., Lloyd, M., Habib, S., Tosha, C., Radu, R.A., Ghyselinck, N.B., Nusinowitz, S. and Bok, D. (2012) Retinoid content, visual responses, and ocular morphology are compromised in the retinas of mice lacking the retinol-binding protein receptor, STRA6. *Invest. Ophthalmol. Vis. Sci.*, **53**, 3027–3039.

17. Amengual, J., Zhang, N., Kemerer, M., Maeda, T., Palczewski, K. and Von Lintig, J. (2014) STRA6 is critical for cellular vitamin A uptake and homeostasis. *Hum. Mol. Genet.*, **23**, 5402–5417.

18. Kelly, M., Widjaja-Adhi, M.A., Palczewski, G. and von Lintig, J. (2016) Transport of vitamin A across blood-tissue barriers is facilitated by STRA6. *FASEB J.*, **30**, 2985–2995.

19. Ramkumar, S., Parmar, V.M., Samuels, I., Berger, N.A., Jastrzebska, B. and von Lintig, J. (2022) The vitamin A transporter STRA6 adjusts the stoichiometry of chromophore and opsins in visual pigment synthesis and recycling. *Hum. Mol. Genet.*, **31**, 548–560.

20. Samardzija, M., Tanimoto, N., Kostic, C., Beck, S., Oberhauser, V., Joly, S., Thiersch, M., Fahl, E., Arsenijevic, Y., von Lintig, J. *et al.* (2009) In conditions of limited chromophore supply rods entrap 11-cis-retinal leading to loss of cone function and cell death. *Hum. Mol. Genet.*, **18**, 1266–1275.

21. Samardzija, M., von Lintig, J., Tanimoto, N., Oberhauser, V., Thiersch, M., Reme, C.E., Seeliger, M., Grimm, C. and Wenzel, A. (2008) R91W mutation in Rpe65 leads to milder early-onset retinal dystrophy due to the generation of low levels of 11-cis-retinal. *Hum. Mol. Genet.*, **17**, 281–292.

22. Rohrer, B. and Crouch, R. (2006) Rod and cone pigment regeneration in RPE65−/− mice. *Adv. Exp. Med. Biol.*, **572**, 101–107.

23. Grune, T., Lietz, G., Palou, A., Ross, A.C., Stahl, W., Tang, G., Thurnham, D., Yin, S.A. and Biesalski, H.K. (2010) Beta-carotene is an important vitamin A source for humans. *J. Nutr.*, **140**, 2268S–2285S.

24. Kelly, M.E., Ramkumar, S., Sun, W., Colon Ortiz, C., Kiser, P.D., Golczak, M. and von Lintig, J. (2018) The biochemical basis of vitamin A production from the asymmetric carotenoid β-cryptoxanthin. *ACS Chem. Biol.*, **13**, 2121–2129.

25. Lindqvist, A. and Andersson, S. (2002) Biochemical properties of purified recombinant human beta-carotene 15,15′-monooxygenase. *J. Biol. Chem.*, **277**, 23942–23948.

26. Rotenstreich, Y., Belkin, M., Sadetzki, S., Chetrit, A., Ferman-Attar, G., Sher, I., Harari, A., Shaish, A. and Harats, D. (2013) Treatment with 9-cisβ-carotene–rich powder in patients with retinitis pigmentosa. *JAMA Ophthalmol.*, **131**, 985–992.

27. Rotenstreich, Y., Harats, D., Shaish, A., Pras, E. and Belkin, M. (2010) Treatment of a retinal dystrophy, fundus albipunctatus, with oral 9-cis-{beta}-carotene. *Br. J. Ophthalmol.*, **94**, 616–621.

28. Meyers, K.J., Johnson, E.J., Bernstein, P.S., Iyengar, S.K., Engelman, C.D., Karki, C.K., Liu, Z., Igo, R.P., Jr., Truitt, B., Klein, M.L. *et al.* (2013) Genetic determinants of macular pigments in women of the carotenoids in age-related eye disease study. *Invest. Ophthalmol. Vis. Sci.*, **54**, 2333–2345.

29. Feigl, B., Morris, C.P., Voisey, J., Kwan, A. and Zele, A.J. (2014) The relationship between BCMO1 gene variants and macular pigment optical density in persons with and without age-related macular degeneration. *PLoS One*, **9**, e89069.

30. Mares, J. (2016) Lutein and zeaxanthin isomers in eye health and disease. *Annu. Rev. Nutr.*, **36**, 571–602.

31. Moon, J., Ramkumar, S. and von Lintig, J. (2022) Genetic dissection in mice reveals a dynamic crosstalk between the delivery pathways of vitamin A. *J. Lipid Res.*, **63**, 100215.

32. Lobo, G.P., Hessel, S., Eichinger, A., Noy, N., Moise, A.R., Wyss, A., Palczewski, K. and von Lintig, J. (2010) ISX is a retinoic acid-sensitive gatekeeper that controls intestinal beta,beta-carotene absorption and vitamin A production. *FASEB J.*, **24**, 1656–1666.

33. Widjaja-Adhi, M.A.K., Palczewski, G., Dale, K., Knauss, E.A., Kelly, M.E., Golczak, M., Levine, A.D. and von Lintig, J. (2017) Transcription factor ISX mediates the cross talk between diet and immunity. *Proc. Natl. Acad. Sci. U. S. A.*, **114**, 11530–11535.

34. Choi, M.Y., Romer, A.I., Hu, M., Lepourcelet, M., Mechoor, A., Yesilaltay, A., Krieger, M., Gray, P.A. and Shivdasani, R.A. (2006) A dynamic expression survey identifies transcription factors relevant in mouse digestive tract development. *Development*, **133**, 4119–4129.

35. Fan, J., Woodruff, M.L., Cilluffo, M.C., Crouch, R.K. and Fain, G.L. (2005) Opsin activation of transduction in the rods of dark-reared Rpe65 knockout mice. *J. Physiol.*, **568**, 83–95.

36. Woodruff, M.L., Wang, Z., Chung, H.Y., Redmond, T.M., Fain, G.L. and Lem, J. (2003) Spontaneous activity of opsin apoprotein is a cause of Leber congenital amaurosis. *Nat. Genet.*, **35**, 158–164.

37. Ridge, K.D., Abdulaev, N.G., Sousa, M. and Palczewski, K. (2003) Phototransduction: crystal clear. *Trends Biochem. Sci.*, **28**, 479–487.

38. Stojanovic, A. and Hwa, J. (2002) Rhodopsin and retinitis pigmentosa: shedding light on structure and function. *Recept. Channels*, **8**, 33–50.

39. Maeda, A., Maeda, T., Golczak, M. and Palczewski, K. (2008) Retinopathy in mice induced by disrupted all-trans-retinal clearance. *J. Biol. Chem.*, **283**, 26684–26693.

40. Chen, Y., Palczewska, G., Mustafi, D., Golczak, M., Dong, Z., Sawada, O., Maeda, T., Maeda, A. and Palczewski, K. (2013) Systems pharmacology identifies drug targets for Stargardt

disease-associated retinal degeneration. *J. Clin. Invest.*, **123**, 5119–5134.

41. Kinoshita, J. and Peachey, N.S. (2018) Noninvasive electroretinographic procedures for the study of the mouse retina. *Curr Protoc Mouse Biol*, **8**, 1–16.

42. Joachimsthaler, A. and Kremers, J. (2019) Mouse cones adapt fast, rods slowly in vivo. *Invest. Ophthalmol. Vis. Sci.*, **60**, 2152–2164.

43. Yokoyama, S. (2000) Molecular evolution of vertebrate visual pigments. *Prog. Retin. Eye Res.*, **19**, 385–419.

44. Redmond, T.M., Poliakov, E., Yu, S., Tsai, J.Y., Lu, Z. and Gentleman, S. (2005) Mutation of key residues of RPE65 abolishes its enzymatic role as isomerohydrolase in the visual cycle. *Proc. Natl. Acad. Sci. U. S. A.*, **102**, 13658–13663.

45. Yan, W., Jang, G.F., Haeseleer, F., Esumi, N., Chang, J., Kerrigan, M., Campochiaro, M., Campochiaro, P., Palczewski, K. and Zack, D.J. (2001) Cloning and characterization of a human beta,beta-carotene-15,15′-dioxygenase that is highly expressed in the retinal pigment epithelium. *Genomics*, **72**, 193–202.

46. Chichili, G.R., Nohr, D., Schaffer, M., von Lintig, J. and Biesalski, H.K. (2005) beta-Carotene conversion into vitamin A in human retinal pigment epithelial cells. *Invest. Ophthalmol. Vis. Sci.*, **46**, 3562–3569.

47. During, A., Doraiswamy, S. and Harrison, E.H. (2008) Xanthophylls are preferentially taken up compared with beta-carotene by retinal cells via a SRBI-dependent mechanism. *J. Lipid Res.*, **49**, 1715–1724.

48. Wassef, L. and Quadro, L. (2011) Uptake of dietary retinoids at the maternal-fetal barrier: in vivo evidence for the role of lipoprotein lipase and alternative pathways. *J. Biol. Chem.*, **286**, 32198–32207.

49. Costabile, B.K., Kim, Y.K., Iqbal, J., Zuccaro, M.V., Wassef, L., Narayanasamy, S., Curley, R.W., Jr., Harrison, E.H., Hussain, M.M. and Quadro, L. (2016) β-apo-10′-carotenoids modulate placental microsomal triglyceride transfer protein expression and function to optimize transport of intact β-carotene to the embryo. *J. Biol. Chem.*, **291**, 18525–18535.

50. Quadro, L., Giordano, E., Costabile, B.K., Nargis, T., Iqbal, J., Kim, Y., Wassef, L. and Hussain, M.M. (2020) Interplay between β-carotene and lipoprotein metabolism at the maternal-fetal barrier. *Biochim. Biophys. Acta Mol. Cell Biol. Lipids*, **1865**, 158591.

51. Zolfaghari, R. and Ross, A.C. (2000) Lecithin:retinol acyltransferase from mouse and rat liver. CDNA cloning and liver-specific regulation by dietary vitamin a and retinoic acid. *J. Lipid Res.*, **41**, 2024–2034.

52. Morshedian, A., Kaylor, J.J., Ng, S.Y., Tsan, A., Frederiksen, R., Xu, T., Yuan, L., Sampath, A.P., Radu, R.A., Fain, G.L. and Travis, G.H. (2019) Light-driven regeneration of cone visual pigments through a mechanism involving RGR opsin in Müller glial cells. *Neuron*, **102**, 1172–1183.e5.

53. Zhang, J., Choi, E.H., Tworak, A., Salom, D., Leinonen, H., Sander, C.L., Hoang, T.V., Handa, J.T., Blackshaw, S., Palczewska, G., Kiser, P.D. and Palczewski, K. (2019) Photic generation of 11-cis-retinal in bovine retinal pigment epithelium. *J. Biol. Chem.*, **294**, 19137–19154.

54. Lobo, G.P., Amengual, J., Baus, D., Shivdasani, R.A., Taylor, D. and von Lintig, J. (2013) Genetics and diet regulate vitamin A production via the homeobox transcription factor ISX. *J. Biol. Chem.*, **288**, 9017–9027.

55. Ramkumar, S., Moon, J., Golczak, M. and von Lintig, J. (2021) LRAT coordinates the negative-feedback regulation of intestinal retinoid biosynthesis from β-carotene. *J. Lipid Res.*, **62**, 100055.

56. Lietz, G., Lange, J. and Rimbach, G. (2010) Molecular and dietary regulation of beta,beta-carotene 15,15′-monooxygenase 1 (BCMO1). *Arch. Biochem. Biophys.*, **502**, 8–16.

57. Mata, N.L., Radu, R.A., Clemmons, R.C. and Travis, G.H. (2002) Isomerization and oxidation of vitamin a in cone-dominant retinas: a novel pathway for visual-pigment regeneration in daylight. *Neuron*, **36**, 69–80.

58. Bhatti, R.A., Yu, S., Boulanger, A., Fariss, R.N., Guo, Y., Bernstein, S.L., Gentleman, S. and Redmond, T.M. (2003) Expression of beta-carotene 15,15′ monooxygenase in retina and RPE-choroid. *Invest. Ophthalmol. Vis. Sci.*, **44**, 44–49.

59. Maeda, T., Perusek, L., Amengual, J., Babino, D., Palczewski, K. and von Lintig, J. (2011) Dietary 9-cis-beta,beta-carotene fails to rescue vision in mouse models of leber congenital amaurosis. *Mol. Pharmacol.*, **80**, 943–952.

60. von Lintig, J., Moon, J., Lee, J. and Ramkumar, S. (2020) Carotenoid metabolism at the intestinal barrier. *Biochim. Biophys. Acta Mol. Cell Biol. Lipids*, **1865**, 158580.

61. Wongsiriroj, N., Jiang, H., Piantedosi, R., Yang, K.J., Kluwe, J., Schwabe, R.F., Ginsberg, H., Goldberg, I.J. and Blaner, W.S. (2014) Genetic dissection of retinoid esterification and accumulation in the liver and adipose tissue. *J. Lipid Res.*, **55**, 104–114.

62. Shen, J., Shi, D., Suzuki, T., Xia, Z., Zhang, H., Araki, K., Wakana, S., Takeda, N., Yamamura, K., Jin, S. and Li, Z. (2016) Severe ocular phenotypes in Rbp4-deficient mice in the C57BL/6 genetic background. *Lab. Invest.*, **96**, 680–691.